17.1.1 X-Ray Emission from SNRs

A SNR is the result of the interaction between the debris from an exploded star and its surrounding medium. The explosion can either arise as the detonation or deflagration of a white dwarf that has exceeded the Chandrasekhar limit as the result of mass accretion from a binary companion (Type Ia) or the gravitational collapse of the core of a massive star that has exhausted its nuclear fuel (Type II, Type Ib, and Type Ic). In the early stages of the remnant evolution, the differences between

J.E. Trümper and G. Hasinger (eds.), *The Universe in X-Rays.*

these explosions can lead to morphological differences, but these begin to blur as the remnant becomes increasingly dominated by the surrounding medium. In both cases the outer layers of the star are ejected with velocity of tens of thousands of kilometers per second. Interaction between the outer envelope and the ambient medium causes the development of a shock front that heats, compresses, and ionizes ambient gas. Undecelerated ejecta catching up with the shell of shocked material produce a reverse shock, so called because it propagates backwards in the ejecta frame of reference (though not in the observer's frame). A contact discontinuity separates the material swept up by the two shocks. For the first few hundred years, during the "free expansion" phase, the forward shock propagates essentially at constant velocity. Once the shock has swept up a mass comparable to that of the ejecta it starts to decelerate, signaling the onset of the so-called adiabatic evolutionary phase. In this phase the cooling time of swept up material exceeds the dynamic time scale, and so the remnant loses very little energy. Its idealized behavior is described by the Sedov–Taylor self-similarity equations. A recent, comprehensive analytic description of SNR evolution under various conditions can be found in [159].

During these two phases, X-ray emission is produced from the collisionally-ionized, shock heated plasma. Both shocks have sufficient velocity to heat the shocked material to high kinetic temperatures; subsequently, collisions with electrons ionizes the gas to predominantly their H-like and He-like states. X-rays are emitted as Bremsstrahlung continuum from the collisionally-heated electrons, plus a rich spectrum of lines from the materials composing the ejecta and the swept-up medium. During the initial phase, lines from the dense ejecta dominate, allowing X-ray observations to probe the properties of the progenitor star via the ejecta abundances and distribution, but as the material in the remnant becomes predominantly swept-up interstellar material, the line spectrum reflects the composition of the interstellar medium. Nonthermal components from electron synchrotron emission arise in central pulsar powered wind nebulae and at the forward shock from electrons accelerated to relativistic energies.

Once the radiative and dynamic timescales become comparable, the remnant enters the radiative or shell forming phase. Newly shocked material radiates its thermal energy and gets swept up into a thin, dense, cool shell. During this phase the shock velocity is too low to produce new X-ray emitting gas, but as described later, X-ray emission still arises from the interior.

17.2.4.1 Expansion Measurements

The availability of X-ray images of SNRs with angular resolution approaching those in the radio and optical made possible the first X-ray measurements of remnant expansion. For a remnant with an average forward shock velocity of 5 000 km s^{-1} at a distance of 3 kpc, the average angular expansion rate is 0.35 arcsec per year. Thus even with the few arc second angular resolution of the early high resolution imagers (Einstein and ROSAT) it became possible to measure global expansion rates of young, nearby remnants over the combined 10–15 yrs baseline spanned by these missions.

The first such measurement was facilitated by a deep ROSAT HRI image of Cas A taken in 1996, that could be used as a template. Koralesky et al. and Vink et al. independently used this observation together with archival ROSAT and Einstein HRI images to perform the first X-ray expansion rate measurements [87,167] . They both found an average expansion rate of $(0.20 \pm 0.01)\%$ per year. The two studies differed on the presence of an azimuthal variation. The expansion rate corresponds to an expansion timescale of ~500 yrs, which can be compared with the ~340 yrs age of Cas A (in 1998). This difference is incompatible with the prediction of a model in which the remnant emission is dominated by ejecta interacting with a circumstellar shell created by a presupernova wind.

Early measurements of global expansion revealed a curious conundrum. In Cas A, Kepler and Tycho, the expansion rate measured in X-rays was roughly twice that measured in the radio [54,55]. For example, the expansion rate of Kepler from the X-ray measurement of 0.239% per year is to be compared with the radio measurement of 0.125% per year. In all three remnants, representing different explosion types and ages, the radio and X-ray features are interspersed, and so a common explanation entailing coincidental surperposition of X-ray filaments passing through the radio filaments is highly unlikely. For Cas A, the problem was compounded by the fact that the cospatial, fast-moving optical knots have an expansion rate 50% still higher than the X-ray. The difference was ascribed to different bands measuring distinct hydrodynamical structures (e.g., [87]), but begged the question of what band measures the true expansion rate.

Detailed kinematic studies using Chandra have helped resolve the issue. DeLaney et al. compared ACIS images of Cas A taken just 2 yrs apart [29]. Their difference map reveals a wide variety of proper motion speeds and directions. They were able to measure the proper motion of hundreds of individual features in addition to measuring the overall expansion of the remnant. They found that the motions throughout the remnant are complex, and cannot be modeled with a homologous expansion (e.g., [159]). The continuum-dominated filaments at the forward shock show a range of expansion rates from 0.02 to 0.33% per year. The median expansion rate of 0.2% per year can be compared with the expected free expansion rate of 0.3% per year to demonstrate that most of the forward shock has undergone significant deceleration. While X-ray ejecta are moving twice as fast as the cospatial radio knots, matched individual X-ray/radio features have the same velocity. Their interpretation of this complex situation is that the small-scale X-ray and radio features in the bright ring (which dominates the emission and thus the global proper motion studies) represent ejecta at various stages of deceleration after passage through the reverse shock. This establishes a velocity gradient from the densest knots, which emit primarily in the optical band, to the radio features which are the most decelerated. Features in all three bands show brightness evolution, however, potentially complicating this straightforward interpretation [30].

In contrast, a similar, preliminary analysis of the X-ray proper motions in Kepler from a pair of Chandra images reveals a mean expansion rate of 0.15% per year, consistent with the radio proper motion [134].

The proper motion study of Cas A also revealed three different classes of X-ray features, separable by their spectral and/or kinematic properties [30]. The Si and Fe dominated ejecta and continuum dominated forward shock filaments have roughly the same proper motion (a mean expansion rate of 0.2% per year), but distinct spatial distributions. This suggests the two components are somehow dynamically coupled. The ejecta knots are associated spatially with the optical fast moving knots, but have been significantly decelerated relative to them, probably as a consequence of lower density. A slow-moving component (0.05% per year) with enhanced low energy emission is apparently associated with the optical quasi-stationary flocculi, and thus might represent a clumpy circumstellar component. Thus, the power of Chandra is beginning to allow us to reconstruct the details of the presupernova environment of Cas A.

Chandra observations have also made possible the first expansion measurement of an extragalactic SNR. By comparing Chandra and ROSAT HRI observations taken 15 yrs previously, Hughes et al. measured the expansion rate of 1E 0102.2-7219 in the SMC of 0.100 ± 0.025 percent per year, corresponding to a shock velocity of $6\,000\,\mathrm{km\,s^{-1}}$ [58].

17.2.4.2 Doppler Measurements

Measurements of radial velocities via Doppler shifts of X-ray lines in SNRs are challenging for even the current generation of instrumentation. While dispersive spectrometers such as crystals and gratings have adequate resolution to resolve velocity broadening produced by motion of a few thousand kilometers per second expected in young SNRs, the motion gets blurred by the finite angular size of the remnants. Nondispersive imaging spectrometers generally lack the spectral resolution to detect the broadening or line centroid shift resulting from radial motion. In only three instances have Doppler shifts been detected: Cas A, as a result of its asymmetric ejecta distribution; 1E 0102.2-7219, because of small size and its well-defined ring shape; and SN 1987A, because of its very small angular size. SN 1987A is discussed in Sect. 17.5.1.

The first measurement of Doppler motions in Cas A was performed using the Einstein FPCS. Markert et al. detected broadening and asymmetry in the Si and S lines [97]. They detected a systematic redshift of the northwest half of the remnant with respect to the southeast, with a mean velocity difference of $1\,820 \pm 290\,\mathrm{km\,s^{-1}}$. Additionally, within each region a Doppler broadening of $5\,000\,\mathrm{km\,s^{-1}}$ was detected. They suggested that the X-ray emission is concentrated in a ring inclined to the plane of the sky, with an expansion velocity greater than $2\,000\,\mathrm{km\,s^{-1}}$.

Subsequent results have largely substantiated these conclusions. Holt et al. constructed the first X-ray Doppler image of Cas A, using the ASCA SIS to measure spatially dependent shifts in the peak of the 1.85 keV Si Heα line [53]. Their map

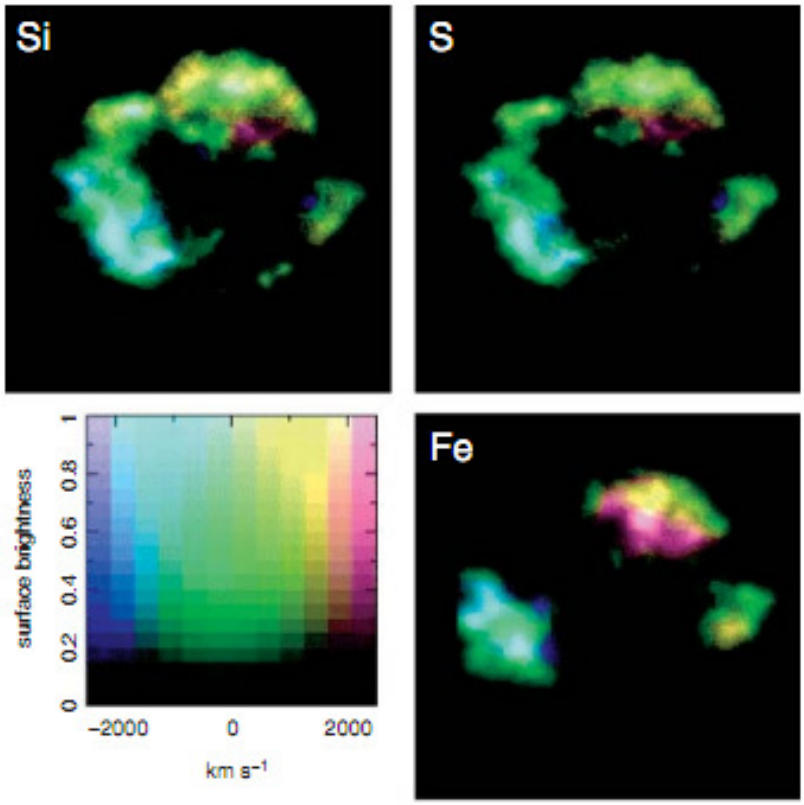

Fig. 17.7 Doppler maps of Si–K, S–K, and Fe–K emission lines in Cas A, extracted from XMM data [178]. The surface brightness of the line emission is color coded with the Doppler velocity using the scheme shown in the bottom left panel

confirmed the Markert et al. finding, but with substantially higher spatial detail. The X-ray emission geometry closely matches that observed in [S II]. Subsequent Chandra and XMM-Newton Doppler maps provided higher resolution views of the radial velocity structures [69, 178]. Willingale et al. used the XMM-Newton Doppler map to reconstruct a three-dimensional view of the Cas A X-ray emission (Fig. 17.7). They infer that the Si and S emission arises exclusively from ejecta and is confined to a narrow shell with radius 100–150 arc seconds. The Fe–K emission is confined in two large clumps, expanding faster and spanning a larger radius range of 110–170 arcsec. They liken these clumps to the ejecta bullets observed in Vela [6].

Flanagan et al. used the Chandra HETG to measure the radial velocities of the line emitting components in the SMC remnant 1E 0102.2-7219, along with their ionization structure (see Sect. 17.2.1.2) [34]. By measuring the different distortions among the dispersed line images, they found Doppler shifts consistent with bulk velocities of $\sim$1 000 km s^{-1}. As for Cas A, the bulk velocities suggest that the emission is confined to a ring, inclined to the line of sight.